

See discussions, stats, and author profiles for this publication at: <https://www.researchgate.net/publication/231389426>

Correlation of Mixture Vapor–Liquid Equilibria with the SPEADMD Model

ARTICLE *in* INDUSTRIAL & ENGINEERING CHEMISTRY RESEARCH · OCTOBER 2008

Impact Factor: 2.59 · DOI: 10.1021/ie800374h

CITATIONS

10

READS

70

3 AUTHORS, INCLUDING:



Amir Vahid

Northwestern University

28 PUBLICATIONS 66 CITATIONS

SEE PROFILE



Jarrell Richard Elliott

University of Akron

100 PUBLICATIONS 1,152 CITATIONS

SEE PROFILE

Correlation of Mixture Vapor–Liquid Equilibria with the SPEADMD Model

Amir Vahid, Amanda D. Sans, and J. Richard Elliott*

Chemical and Biomolecular Engineering Department, The University of Akron, Akron, Ohio 44325-3906

The present work examines the accuracy of the SPEADMD molecular simulation methodology in correlating experimental data relative to a standard low-pressure database for testing VLE models. The database contains 104 binary systems categorized according to polarity and ideality. Although the database is somewhat small, it covers a broad range of chemical functionality, including halocarbons and carboxylic acids as well as hydrocarbons and alcohols. Six models were tested and compared for their characterization of these mixtures. Four standard models were evaluated to establish a basis for comparison: the Margules, NRTL, PR, and PRWS models. The SPEADMD model was evaluated in three forms. In its elementary form, the SPEADMD model includes ~10% deviations in vapor pressure because of the application of transferable potential functions in the molecular model. An alternative model is developed on the basis of SPEADMD combined with corrected vapor pressures and customized self-interaction parameter for pure compounds. This alternative is referred to as the SPEADCI model, in which CI stands for customized interactions. Results show that SPEADCI model provides accuracy similar to the NRTL and PRWS models, even though it includes only one adjustable parameter per binary system, whereas the NRTL model includes two and the PRWS models include three. Deviations in correlated bubble point pressure are roughly 1–2% for these models. The SPEADMD models have the advantage that transferable potentials can be applied for solvation interactions that are similar to the Kamlet-Taft interaction parameters.

1. Introduction

Accurate vapor–liquid equilibrium (VLE) estimation is important for many chemical processes, most notably distillation. Often, experimental data do not exist for VLE in the temperature range of interest. Therefore models to predict VLE have become important. The most basic model for VLE is Raoult's Law, $y_i P = x_i P_i^{\text{sat}}$, where P is pressure, P_i^{sat} , x_i , and y_i are the vapor pressure and liquid and vapor mole fractions component of i , respectively. Raoult's Law assumes ideal mixing for all systems. However, most mixtures are nonideal, and thus more sophisticated methods are needed to explain mixture behavior. Two methods are commonly used for calculating VLE. The distinction between them is in the way the fugacity (ϕ) of the liquid is calculated. The fugacity of the vapor phase is always calculated using an equation of state (EOS). The fugacity of the liquid phase can be calculated by using either the same EOS used for the gas or by the activity coefficient (γ) method.¹

The SPEADMD model is based on Step Potential Equilibria And Discontinuous Molecular Dynamics.² It provides a bridge between molecular simulation methodology and a conventional approach to engineering phase behavior models. By discretizing the intermolecular potential model into a series of steps, a combination of discontinuous molecular dynamics (DMD) simulation and thermodynamic perturbation theory (TPT) can be adapted to achieve a high degree of leverage from each simulation.³ The SPEADMD model begins with molecular simulation of pure fluids and mixtures. Simulation of every pure fluid is necessary to characterize the TPT contributions. Because of the adaptation of TPT for temperature effects, simulations of the reference fluid over the entire density range provide a complete EOS, customized for the particular molecular model at hand through the configurations generated by its particular size and shape. In principle, treating mixtures requires simulating each binary mixture over a range of compositions and densities.

Gray and Elliott performed this kind of analysis for a broad range of binary mixtures and identified consistent trends in the perturbation contributions.⁴ These trends can be expressed in the form of mixing rules with one binary interaction parameter (BIP) per binary system. Consequently, it is feasible to assume the validity of these mixing rules without exhaustively simulating every binary mixture, an added form of leverage derived from the SPEADMD approach. It is necessary to simulate each binary system to develop the connection between the site–site intermolecular potential and the macroscopic BIP, but explicitly making that connection is unnecessary when assessing the accuracy of the SPEADMD model for correlating a large VLE database. Hence the present work focuses on correlating the macroscopic BIPs in order to assess the level of accuracy that can be expected for an approach based on molecular simulations. Relating the macroscopic BIPs to the site–site BIPs would enable prediction of VLE solely on the basis of molecular structure. Developing predictive capability will be the subject of future work.

2. Activity Models

The simplest form of the activity coefficient model uses only one parameter and is called the Margules two-suffix equation $G^{\text{ex}} = Ax_1x_2$, where G^{ex} is the Gibbs excess energy, A is the Margules constant, and x_1 and x_2 are the liquid mole fractions for the first and second components. Danner and Gess reported the Margules constant for all systems in the database of their original publication.⁵ One advantage of the Margules constant is that it provides a simple indicator of whether G^{ex} is positive or negative. Negative values of G^{ex} are relatively uncommon and therefore indicate behavior that is often interesting. Activity coefficient models more commonly use two or more parameters for each pair of components in the mixture. Two examples of well-known activity coefficient models with multiple parameters are NRTL (Non-Random-Two-Liquid model),⁶ and UNIQUAC (UNIversal QUasi Chemical model).⁷ The 2–3 parameters for NRTL and 2 parameters of UNIQUAC are obtained from fitting

* To whom correspondence should be addressed. E-mail: jelliott@uakron.edu.

binary mixture information at the molecule-molecule level. Another common activity model is the UNIFAC (UNiversal Functional Activity Coefficient) model.⁸ UNIFAC uses group contributions, which can be found in group tables. In group contribution methods, the mixture can be treated as a mixture of groups instead of a mixture of molecules. For example, isopropanol consists of 2(CH₃) + 1(CH) + 1(OH).⁹ UNIFAC is not comparable in the present study because the binary interaction parameters (BIPs) of the SPEADMD model are presently correlated to experimental data on a molecule-molecule basis, neglecting the site-site BIPs. Future work will focus on optimizing site-site BIPs and that work will be comparable to UNIFAC. The activity coefficient model, with suitable parameters, can describe the VLE of very nonideal systems. The main disadvantage of the activity coefficient model is that the critical point, where the vapor and liquid phases are indistinguishable, cannot be predicted because the liquid and vapor phases use different models that cannot converge mathematically.¹

3. EOS Models

The EOS models are based on the classic van der Waals equation, such as the Peng–Robinson EOS, extended from the virial equation, or derived from statistical mechanical theory. EOS models effectively interpolate between pure fluids by applying mixing rules. The main assumption of the mixing rules is that the parameters for the EOS of the mixture can be calculated from some combination of the parameters for the EOS of the pure fluids. For example, the generic combining rule for the mixture coefficients in van der Waals type models, a_{ij} and b_{ij} , are calculated from the pure component parameters, a_{ii} and b_{ii} , usually using the following forms $a_{ij} = \sqrt{a_{ii}a_{jj}(1 - k_{ij})}$ or $b_{ij} = 0.5(b_i + b_j)(1 - l_{ij})$, where k_{ij} and l_{ij} are binary interaction parameters (BIPs) found by fitting the EOS predictions to experimental data. VLE or G^{ex} EOS mixing rules can also be generalized by taking the limit of the EOS at a particular pressure (e.g., $P \rightarrow \infty$ or $P = 0$) and applying an activity model like NRTL or UNIQUAC to the liquid under those conditions.¹ The resulting EOS model has the flexibility to fit mixture behavior like an activity model but retains the capability to compute properties in all phase space, including the critical region. An example of an EOS in combination with a generalized mixing rules is the Peng–Robinson EOS with Wong–Sandler mixing rules (PRWS).¹⁰ SPEADMD is an EOS model with its own mixing rules developed by simulating many mixtures to determine viable rules for interpolating between state points.

4. SPEADMD-EOS and SPEADCI Models

The SPEADMD and SPEADCI models use the same mixing rules for the EOS; the only difference is that SPEADCI uses a vapor pressure correction. The SPEADMD model's first role is as a molecular simulation, which predicts pure fluid properties such as vapor pressure and liquid density. Consequently, SPEADMD has large vapor pressure deviations compared with NRTL or PRWS, which simply apply experimental values of vapor pressure. The mixture simulations are more computationally intensive than the pure fluid simulations, so mixtures are simulated only as needed. Instead, mixing rules are used, which are based on simulations of many mixtures and assumed to provide accurate interpolation capability even when they have not been tested for every specific mixture. The most general form of the SPEADMD EOS for pure fluids is written as

$$Z = 1 + Z^{\text{ref}} + Z^{\text{att}} + Z^{\text{assoc}} \quad (1)$$

The EOS is actually the derivative of the Helmholtz free energy with $Z^{\text{ref}} = Z_0$ and $Z^{\text{att}} = (Z_1/T) + (Z_2/T^2)$ (NOTE: $1 = Z^{\text{ig}}$ so $(A - A^{\text{ig}})/RT \approx \int (Z - Z^{\text{ig}}) d\rho/\rho$). Rearranging the equation and substituting gives the following result

$$\begin{aligned} Z(\eta) - 1 &= Z_0 + \frac{Z_1}{T} + \frac{Z_2}{T^2} + Z^{\text{assoc}} \eta \left(\frac{d(A - A^{\text{ig}})/RT}{d\eta} \right) \\ &= \left[\eta \left(\frac{dA_0}{d\eta} \right)_{T,y} \right] + \eta \frac{dA_1}{d\eta} \left(\frac{1}{T} \right) + \eta \frac{dA_2}{d\eta} \left(\frac{1}{T} \right)^2 + \eta \frac{dA^{\text{assoc}}}{d\eta} \end{aligned} \quad (2)$$

where the Helmholtz free energy is defined by

$$\frac{A - A^{\text{ig}}}{RT} = A_0 + \left(\frac{A_1}{T} + \frac{A_2}{T^2} \right) + A^{\text{assoc}} = \frac{A^{\text{rep}}}{RT} + \frac{A^{\text{att}}}{RT} + \frac{A^{\text{assoc}}}{RT} \quad (3)$$

The term first term A^{ig} is the Helmholtz free energy (A) for the ideal gas, A_0 is for the purely repulsive fluid, A_1 and A_2 the first- and second-order perturbation terms respectively which describe the attractive forces of the fluid, and A^{assoc} is for association of fluids. The reference fluid is described by

$$A_0 = \int \frac{Z_0 - 1}{\eta} d\eta \quad (4)$$

$$Z_0 = \frac{1 + z_1\eta + z_2\eta^2 + z_3\eta^3}{(1 - \eta)^3} \quad (5)$$

where Z_0 is the compressibility factor for the reference fluid and follows the Carnahan–Starling¹¹ equation of state for hard spheres.

The attractions in the fluid are described by the first- and second-order perturbation terms, which are

$$A_1 = a_{11}\eta + a_{12}\eta^2 + a_{13}\eta^3 + a_{14}\eta^4 \quad (6)$$

$$A_2 = \frac{a_{21}\eta + a_{22}\eta^2 + a_{23}\eta^3 + a_{24}\eta^4}{1 + 500\eta^4} \quad (7)$$

The last term that makes up the equation of state is the Helmholtz free energy of association, which is defined by

$$A^{\text{assoc}} = \sum_i x_i \left[\sum_j \ln X_i^{A_j} + \frac{(1 - X_i^{A_j})}{2} + \sum_j \ln X_i^{D_j} + \frac{(1 - X_i^{D_j})}{2} \right] \quad (8)$$

$$1 - X_i^{A_j} = X_i^{A_j} \sum_k x_k \sum_i X_k^{D_l} a_{ik}^{A_j D_l} 1 - X_i^{D_j} = X_i^{D_j} \sum_k x_k \sum_i X_k^{A_l} a_{ik}^{D_j A_l} \quad (9)$$

$$\alpha_{ik}^{A_j D_l} = \frac{\rho(1 - \eta/2)}{(1 - \eta)^3} K_{ik}^{A_j D_l} [\exp(\beta \epsilon_{ik}^{A_j D_l}) - 1] \quad (10)$$

where ρ is the molar density, η is the packing fraction, $K_{ik}^{A_j D_l}$ is the molar acceptor–donor bonding volume, $\epsilon_{ik}^{A_j D_l}$ is the molecular acceptor–donor bonding energy, and $\beta = 1/k_B T$ the reciprocal temperature with the Boltzmann constant k_B . For example, $\epsilon_{ik}^{A_j D_l}$ refers to the energy of bonding between the j th acceptor on the i th molecule and the l th donor on the k th molecule. The parameters used to describe the EOS are referred to as ParmsTpt. These parameters include the coefficients for the reference fluid Z_0 ($z_1^{\text{ref}}, z_2^{\text{ref}}, z_3^{\text{ref}}$), the coefficients for the first order contribution A_1 ($a_{11}, a_{12}, a_{13}, a_{14}$), and the coefficients for the second order contribution A_2 ($a_{21}, a_{22}, a_{23}, a_{24}$). These parameters are given in the Supporting Information, Table C4. The ParmsTpt file is generally evolving as the characterizations of site–site interactions are continuously improved, so it is necessary to specify the parameters applied in this work in order

to make it reproducible. Nevertheless, the results reported here are dominated by the vapor pressure accuracy and the estimated molecular volumes. Because these values are not expected to change substantially, it is expected that the results reported here are substantially equivalent to results with updated values of ParmsTpt.

The mixing rules for the SPEADMD EOS (below) were developed by simulating many mixtures and examining the trends. Gray and Elliott⁴ found that the entropy and disperse energy of mixing (A_0 , A_1 , A_2) all followed the van der Waals 1-fluid rule as the interpolation function between state points. In this way, the statistical average from the molecular simulation is retained as the underlying definition of the thermodynamics.

4.1. Athermal Entropy of Mixing. Noting that $A \equiv U - TS$, and $(U - U^{\text{is}}) = 0$ for the reference fluid, we observe that $A_0/RT = -S_0/R$, where S_0 is the athermal entropy. Equation 4 shows that these entropies are computed by thermodynamic integration, which is inherently more precise than the differentiation that is often applied in evaluating the entropy by molecular simulation. The purpose of the mixing rule is to retain this precision while interpolating between simulated state points. The entropy of mixing from simulation was overestimated by the default mixing rule, thus the mixing rule needed a binary interaction parameter (BIP) for entropy of mixing, $k_{ij}^S = (-0.022(b_1 + b_2)/(1.987 \times 298))(\delta_2^S - \delta_1^S)^2$, in order to match simulation results.

$$\frac{-S_0^{\text{ss}}}{R} = \frac{\chi^S(\eta)\Phi_1\Phi_2b}{R} \quad (11)$$

$$\chi^S \equiv \left[\frac{2S_{012}}{(b_1b_2)^{1/2}} - \left(\frac{S_{011}}{b_1} + \frac{S_{022}}{b_2} \right) \right] = -(\delta_2^S - \delta_1^S)^2 - 2(\delta_1^S\delta_2^S)k_{ij}^S \quad (12)$$

where the molar volume is $b = \sum x_i b_i$; $b_i = N_A v_i^{\text{eff}}$, the packing fraction is $\eta = b\rho$; $\rho \equiv$ molar density; $N_A \equiv$ Avogadro's number; $\delta_i^S \equiv (S_{0ii}/b_i)^{1/2}$; $S_{0ij} = S_{0ji} \equiv (S_{0ii}S_{0jj})^{1/2}(1 - k_{ij}^S)$.

Here the excess properties are calculated at constant packing fraction. Further note that χ^S is a function of packing fraction, because S_{0ii} is a function of η . In principle, k_{ij}^S is a binary parameter that may vary according the particular binary system of interest. However, Gray and Elliott⁴ found that the approximation of $k_{ij}^S = (-0.022(b_1 + b_2)/(1.987 \times 298))(\delta_2^S - \delta_1^S)^2$ provided near quantitative accuracy for all mixtures studied, including aromatic, aliphatic, and alcohol mixtures with volume ratios as large as 10:1. To appreciate how this is possible, one must recognize that S_0 is purely repulsive. The attractive effects contribute as perturbations. Therefore, contributions to S_0 are simply related to effects of size and shape. By accounting for the entropy density through the entropic solubility parameter, a universal correlation of k_{ij}^S becomes feasible, at least for mixtures with volume ratios of 10 or less. A small inconsistency in S_0 may arise in the infinite chain limit for polymer solutions. We are currently working to resolve this by simulating mixtures with very long chains. All mixtures in the Danner–Gess database are within the range of molecular sizes that we have previously simulated where eqs 11 and 12 have been demonstrated to be accurate.

4.2. Energy of Mixing. The van der Waals excess function can be derived from the van der Waals mixing rule as follows, taking the first-order term as an example. The AM (first order perturbation term) for the mixture is defined as

$$AM = \frac{x_1^2 b_1 A_{111} + 2x_1 x_2 A_{112}(b_1 b_2)^{1/2} + x_2^2 b_2 A_{222}}{x_1 b_1 + x_2 b_2} \quad (13)$$

where A_{1ii} is for the pure fluid and $A_{1ij} \equiv (A_{1ii}A_{1jj})^{1/2}(1 - k_{ij}^{A1})$, k_{ij}^{A1} is the BIP for A_1 , and x_i is the mole fraction of component i . The A_1 term for the ideal solution is

$$AM^{\text{is}} = (x_1 A_{111} + x_2 A_{122}) \left(\frac{x_1 b_1 + x_2 b_2}{x_1 b_1 + x_2 b_2} \right) = \frac{x_1^2 b_1 A_{111} + x_1 x_2 (b_2 A_{111} + b_1 A_{122}) + x_2^2 b_2 A_{122}}{x_1 b_1 + x_2 b_2} \quad (14)$$

For any property, the excess property is the difference between the property for the mixture and the property for the ideal solution, so for AM^E

$$AM^E = \frac{AM}{RT} - \frac{AM^{\text{is}}}{RT} = \frac{2x_1 x_2 [A_{112}(b_1 b_2)^{1/2} - 0.5(b_2 A_{111} + b_1 A_{122})]}{x_1 b_1 + x_2 b_2} = \chi^{A1} \Phi_1 \Phi_2 b \quad (15)$$

The form to the far right is the familiar van der Waals form, where Φ_i is the volume fraction for the i th component, and

$$\chi^{A1} \equiv \left[\frac{2A_{112}}{(b_1 b_2)^{1/2}} - \left(\frac{A_{111}}{b_1} + \frac{A_{122}}{b_2} \right) \right] = \frac{(\delta_2^{A1} - \delta_1^{A1})^2 + 2(\delta_1^{A1} \delta_2^{A1})(1 - k_{ij}^{A1})}{(b_1 b_2)^{1/2}} \quad (16)$$

where $\delta_i^{A1} \equiv (A_{1ii}/b_i)^{1/2}$

Basically, molecules are composed of sites and these sites interact with each other. Therefore, if we characterize the site–site interactions, the molecule–molecule interactions can readily be predicted. Gray and Elliott⁴ also showed that the energy of mixing could be described equally well with a molecule–molecule BIP, k_{ij}^{mm} , or a site–site BIP, k_{ij}^{ss} . The k_{ij}^{ss} is more transferable, but requires a more extensive global optimization to characterize. Because the Danner–Gess database is not comprehensive enough for the global approach and k_{ij}^{mm} has the capability to characterize the simulation results, this work focuses only on the k_{ij}^{mm} . The site–site approach has been implemented by Sans and Elliott¹² for perfluorinated hydrocarbons. To achieve a completely predictive model, future study will focus on prediction using the global approach. In this way, transferable site–site interactions (k_{ij}^{ss}) must be refined to permit prediction of the molecule–molecule interactions (k_{ij}^{mm}).

Accurate vapor pressure prediction is necessary for accurate VLE predictions. Unfortunately, the SPEADMD predictions of vapor pressure can have 10–20% error, skewing the comparison to standard activity models that assume the vapor pressure as given. The reason that a model like SPEADMD contains 11 parameters (eqs 5–7 but cannot give accurate predictions of vapor pressure is that all of these parameters are fitted to simulation results, not experimental data. For instance, the coefficients of eq 5 are obtained by correlating compressibility factors of reference fluids from simulation. Also, as discussed by Elliott et al.,¹³ the main reason that SPEADMD can have 10–20% AAD in the vapor pressure is transferability. In contrast to models like PRWS, the SPEADMD model applies a transferable characterization of site–site interactions that is not compound-specific. In general, transferability is a reasonable approximation but still an approximation, which results in deviation from experimental vapor pressure data. An alternative can be formulated to customize the SPEADMD model for specific compounds.

In this alternative, we alter the strength of the attractive perturbation by multiplying it by a customized interaction parameter. That is

$$A^{\text{att}} = A_{\text{trans}}^{\text{att}}(1 - k_{ii}) \quad (17)$$

where $A_{\text{trans}}^{\text{att}}$ is the attractive Helmholtz energy computed from the transferable potentials and $k_{ii} = k_{ii}^0 + k_{ii}^1\eta$ is the customized interaction parameter.

We designate this model as SPEADCI, which refers to the customized interaction parameter. In this manner, SPEADCI has two compound specific parameters, k_{ii}^0 and k_{ii}^1 . The SPEADCI model is necessary to achieve a consistent comparison to the other activity models by eliminating the vapor pressure error derived from the transferability assumption.

The fugacity of the mixture is calculated using the following equation in combination with the previously mentioned mixing rules.⁹

$$\ln\left(\frac{\hat{f}_i}{y_i P}\right) = \left(\frac{\partial(\bar{G} - \bar{G}^{\text{ig}})/RT}{\partial n_i}\right)_{T,P,n_j \neq i} = \left(\frac{\partial(\bar{A} - \bar{A}^{\text{ig}})/RT}{\partial n_i}\right)_{T,\bar{V},n_j \neq i} - \ln(Z) \quad (18)$$

5. Evaluation of Vapor Liquid Equilibrium Using the Danner–Gess Standard Database

Hundreds of VLE models have been proposed and more are proposed every day. It is not uncommon for authors of new models to evaluate their methods with a selected database. Because every author uses a different database, it becomes difficult to compare methods to each other. Furthermore, evaluation of VLE models requires a reliable data set. Choosing which VLE systems to use for testing the accuracy of predictions is difficult because of the large amount of data available, some of which may be of unknown reliability or not clearly categorizable. For these reasons, a standard low pressure database for testing VLE models was developed by Danner and Gess.⁵ The database contains 104 binary systems which have been categorized according to polarity and ideality. The general classification of the VLE systems is given in Table 1. Special care was taken to make sure the data were (1) thermodynamically consistent, (2) classified in such a way that new systems could be assigned easily to one of the classes, and (3) evenly distributed among and within the systems' entire composition range.

In the present work, the data were analyzed in the manner recommended by Danner and Gess, predicting y values based on optimizing P – T – x consistency and then testing accuracy of the model by deviations between computed and experimental P and y values. Four models were compared: NRTL, PRWS, SPEADMD, and SPEADCI. For completeness, the equations for the well-known models, NRTL and PRWS, are given in Appendix A of the Supporting Information.

The best fit for all parameters is determined by minimizing the percent absolute average deviation in bubble point pressure (%AADbp). We minimize the sum of squared error by using

Table 1. Classifications by Danner and Gess for VLE

VLE Classification	abbreviation	no. of systems
nonpolar–nonpolar	NPLNPL	16
nonpolar–weakly polar	NPLWKP	14
nonpolar–strongly polar	NPLSTP	24
weakly polar–weakly Polar	WKPWKP	8
weakly polar–strongly polar	WKPSTP	13
strongly polar–strongly Polar	STPSTP	13
aqueous–strongly polar	VSTSTP	5
immiscible systems	IMMIS	6
carboxylic acid systems	CARBOX	5

Table 2. Summary of %AAD by Class for Each Model

class	NRTL	PRWS2	PRWS3	PRWS4	SPEADMD	SPEADCI
NPLNPL	0.25	0.69	0.64	0.62	3.28	2.08
NPLWKP	0.36	1.42	0.99	0.86	3.25	1.97
NPLSTP	0.53	1.29	0.92	0.81	4.10	1.73
WKPWKP	0.66	1.13	0.90	0.79	5.79	1.30
WKPSTP	0.58	1.12	0.91	0.90	3.12	2.01
STPSTP	0.52	1.31	1.22	1.19	5.19	2.70
VSTSTP	0.90	1.58	1.33	0.83	3.12	2.67
IMMIS	1.53	4.21	2.75	2.18	7.18	6.06
CARBOX	0.79	3.24	2.45	1.55	7.31	1.56
AVERAGE	0.57	1.46	1.12	0.96	4.70	2.45

Levenberg–Marquardt algorithm.¹⁴ To estimate standard errors, we apply the Ralston–Jennrich method.¹⁵

Two methods were used to quantify the error in prediction. The first is the %AADbp. The second is the standard error as defined by Danner and Gess⁵ (SEDG). The %AADbp and SEDG are defined by the following equations, respectively:

$$\% \text{AADbp} = \frac{1}{n_{\text{pts}}} \sum_{i=1}^{n_{\text{pts}}} \frac{|P_i^* - P_i|}{P_i} \quad (19)$$

$$\text{SEDG} = \left[\sum_{i=1}^{n_{\text{pts}}} \frac{(G^{\text{E}}/RT - G^{\text{E}*}/RT)^2}{(n_{\text{pts}} - 1)} \right]^{1/2} \quad (20)$$

where n_{pts} is the number of data points. The asterisk (*) denotes a predicted value, experimental values have no asterisk. The predicted G^{E} is calculated by the following.

$$G^{\text{E}} = \sum_{i=1}^n x_i \bar{G}_i^{\text{E}} = RT \sum_{i=1}^n x_i \ln \gamma_i \quad (21)$$

$$\gamma_i = \frac{y_i P}{x_i P_i^{\text{sat}}} \quad (22)$$

where \bar{G}_i^{E} is the partial molar Gibbs excess energy and x_i and y_i are the liquid and vapor mol fractions of component i respectively. γ_i is the activity coefficient of component i , and P_i^{sat} is the vapor pressure of component i .

6. Results and Discussion

The SPEADCI method typically uses one BIP, whereas NRTL has 2–3 BIPs. The PRWS model has two, three, or four parameter models called PRWS2, PRWS3, and PRWS4, respectively. The parameters in the PRWS2 model are the τ_{12} and τ_{21} of the NRTL mixing rule. PRWS3 adds k_{ij} . The PRWS4 model keeps $k_{ij} = 0$, but makes τ_{12} and τ_{21} temperature-dependent. Extra parameters complicate a model, so the improvement in bubble pressure error must be examined to justify adding a parameter. The SPEADMD and SPEADCI models also have extra parameters to characterize anomalous solvation for a few specific systems, as discussed below. The BIPs of all systems for the EOS studied are given in Appendix B of the Supporting Information, including NRTL, PRWS2, PRWS3, PRWS4, SPEADMD, and SPEADCI.

The VLE models are compared by the classification system of Danner and Gess in Table 2 based on %AADbp and in Table 3 based on SEDG. The NRTL model consistently performs best for all classifications, with an overall %AAD = 0.57 which is half-that of the other models. In general, the %AADbp is below 1% for the NRTL, PRWS3, SPEADCI methods, whereas the SPEADMD EOS method has roughly 10 times larger error than any of the methods based on activity models and/or customized interactions. The larger error (6%) for the SPEADMD model is expected because of the error in generalized vapor pressure

Table 3. Summary of SEDG by Class for Each Model

class	NRTL	PRWS2	PRWS3	PRWS4	SPEADMD	SPEADCI
NPLNPL	0.004	0.015	0.015	0.023	0.0701	0.0339
NPLWKP	0.005	0.028	0.026	0.025	0.0352	0.0321
NPLSTP	0.008	0.036	0.027	0.046	0.0645	0.0316
WKPWKP	0.009	0.024	0.025	0.023	0.0117	0.0109
WKPSTP	0.007	0.039	0.040	0.050	0.0639	0.0408
STPSTP	0.007	0.026	0.026	0.044	0.0701	0.0525
VSTSTP	0.019	0.059	0.056	0.029	0.0320	0.0254
IMMIS	0.020	0.144	0.112	0.155	0.0649	0.0585
CARBOX	0.010	0.052	0.054	0.059	0.2095	0.1063
average	0.008	0.038	0.034	0.044	0.0691	0.0436

correlation from simulation results. SPEADMD EOS has an average of about ~9% error in vapor pressure for these compounds, so the error of 6% for VLE is actually better than what might be expected. The smaller deviation for VLE may be caused by the vapor pressures implicit in the database being near the boiling temperature, which is generally more accurately correlated by the SPEADMD EOS. Furthermore, the smaller deviation for VLE may be an artifact of the regression procedure, which minimizes %AADbp regardless of the model's vapor pressures. The listing of vapor pressure and liquid density errors for each molecule in the database is located in Appendix C of the Supporting Information. Also this appendix includes the results for predicted value of the normal boiling point and acentric factor of each individual compound.

The results for each system for the various methods are compared in Table 3 based on SEDG and in Table 4 based on %AADbp. For a few systems, the SPEADCI are roughly the same as the SPEADMD error. This similarity is because the SPEADMD vapor pressure for the pure components happened to be very accurate in the temperature range of the VLE, thus the vapor pressure correction offered by SPEADCI was of no benefit for these systems. The systems with high vapor pressure error from SPEADMD were greatly benefited by using the SPEADCI vapor pressure correction.

For all models, the error for the IMMIS class is much higher than for the other classes, roughly twice the %AAD. However, SPEADCI with a %AAD ~3 times that of other models is relatively inaccurate in characterizing immiscible systems. This large error is primarily due to mixtures containing nitroethane and the water + phenol system. These failures indicate that additional work with SPEADMD is necessary to understand the peculiarities of the nitrate systems and to characterize them accurately. The VLE can be improved for these challenging systems by refining the characterization of solvation. The nature of the detailed analysis is illustrated in the following section for several systems. Extending such detailed analysis to every system in the database is beyond the scope of the current study since the present study is focused on correlating VLE systems from pure compounds in a straightforward and simple manner. A detailed listing based on SEDG is also available upon request from the authors.

It is worth mentioning that we also have analyzed the γ - φ approach of the SPEADMD model, i.e., SPEADMD γ ¹³ model for the Danner-Gess database (Supporting Information, Table B2), but we decided to not consider it in this paper. Basically, for carboxylic acids, the assumption of an ideal vapor phase, i.e., $Z^{\text{vap}} = 1$ and $\varphi_i^{\text{V}} = 1$, is no longer valid because of strong association in the vapor phase. Hence, SPEADMD γ model leads to difficulty when equating vapor and liquid fugacities. The SPEADCI method avoids this difficulty by applying a consistent model to both vapor and liquid fugacities and its accuracy for vapor pressure is comparable to that of the SPEADMD γ method.

6.1. Detailed Analysis of Several Illustrative Systems.

Considering the added number of BIPs with NRTL, PRWS2, PRWS3, SPEADMD, and SPEADCI performed well. Recall that NRTL has two BIPs and PRWS3 has three BIPs, whereas SPEADMD and SPEADCI have only one BIP. All models do well at characterizing the G^{E} for systems that are nonpolar-nonpolar. For example, Figure 1 shows the VLE and G^{E} for a typical nonpolar-nonpolar system, octane + ethylbenzene using the SPEADCI model. Note that the skewness of the Gibbs Excess function is fairly steady even when $k_{ij} = 0$. As k_{ij} is varied, the magnitude of G^{ex} changes, but not the skewness. The value of $k_{ij} = 0.0032$ is optimal for the VLE of this system. The %AADP for NRTL, PRWS3, SPEADMD, and SPEADCI were 0.20, 0.13, 0.30, and 0.29, respectively.

There are a few systems for which the SPEADCI approach is inferior to the SPEADMD EOS model. Examples of these systems are isopropanol (IPA) + water and 1,4-dioxane + methanol. For IPA + water, the discrepancy in error is small and random. Because neither model really fits well, it so happens that the vapor pressure coincidentally favors the SPEADMD over SPEADCI by a slight amount. The other system is complicated by weak molecular interactions. There are two types of complex molecular interaction, solvation and association. Solvation is complexation between molecules of different components. Association is complexation between molecules of the same component. Hydrogen bonding in alcohols is an example of association. Note that the solvation interaction treated by a transferable approach as discussed in our previous work.¹³ For instance, in the case of alcohol-amine interaction the synergistic bonding interactions are more strongly favorable than expected by the general guideline. Therefore, a transferable approach is needed for considering the solvation energy between alcohol-amine sites. SPEADCI is able to perform well with only one parameter because Wertheim's theory for hydrogen bonding accounts for most of the variation in the Gibbs Excess energy (G^{E}), leaving a relatively small correction to be covered by the BIP in SPEADCI. The solvation effect can be refined to improve the SPEADMD models. The SPEADMD models represent solvation and association using donor and acceptor sites defined by bonding volume K^{AD} and bonding energy ϵ^{AD} described in previous equations. The number of donors does not have to equal the number of acceptors, which is important for describing molecules that can solvate, but not associate.

A classical example of solvation is provided by the acetone+chloroform system, illustrated in Figure 2. In Figure 2, the deviation from Raoult's law is positive when the BIP (k_{ij}) is set to zero with zero solvation energy. Applying a solvation energy of 2.15 kcal/mol provides an accurate explanation of the system both in terms of the empirical deviations and the qualitative chemical description. The chemical description is that the polarities of these species lead to a solvation complex. Note that the C-H stretch in chloroform is distinct from what is normally meant by a "hydrogen bond." A similar result is found for diethyl ether + chloroform with a solvation energy of 1.5 kcal/mol. These solvation energies can be applied transferably to other ketone, ether, and halocarbon interactions, similar to the Kamlet-Taft parameters.¹³

Several systems in Table 3 relate to alcohol + amine interactions. These provide examples of hydrogen bonding species that strongly solvate. Fundamentally, the alcohols are somewhat more acidic than basic and the amines are more basic than acidic, as reflected by their Kamlet-Taft parameters. This explains why their solvation interactions lead to negative deviations from Raoult's law. Detailed analysis of alcohol-amine

Table 4. Detailed Listing of VLE Systems with %AAD in Bubble Pressure

system				% AAD P			
ID1	ID2	component 1	component 2	NRTL	PRWS3	SPEADMD	SPEADCI
Nonpolar/Nonpolar Ideal Systems							
501	502	benzene	toluene	0.06	0.46	4.86	0.95
17	504	heptane	ethylbenzene	0.06	0.29	0.20	0.15
27	504	octane	ethylbenzene	0.20	0.13	0.30	0.29
234	502	1-heptene	toluene	0.38	1.05	4.34	0.71
17	507	heptane	<i>p</i> -xylene	0.06	0.52	3.92	0.27
501	137	benzene	cyclohexane	0.15	0.36	3.08	0.42
105	501	methylcyclopentane	benzene	0.03	0.35	1.94	0.29
137	502	cyclohexane	toluene	1.05	1.51	4.18	1.19
309	214	isoprene	2-methyl-2-butene	0.09	0.54	10.47	0.86
1864	502	hexafluorobenzene	toluene	0.52	0.56	5.80	1.34
1501	501	tetrachloromethane	benzene	0.16	0.33	0.64	0.33
1938	137	carbon disulfide	cyclohexane	0.06	1.35	1.52	1.37
1938	104	carbon disulfide	cyclopentane	0.08	0.71	1.07	0.97
1938	1501	carbon disulfide	tetrachloromethane	0.21	0.71	1.84	1.24
Nonpolar/Nonpolar Nonideal Systems							
1864	507	hexafluorobenzene	<i>p</i> -xylene	0.79	1.02	7.08	1.84
1864	137	hexafluorobenzene	cyclohexane	0.10	0.36	1.32	0.55
		average nonpolar/weakly polar		0.25	0.64	3.28	0.80
Nonpolar/Weakly Polar Ideal Systems							
502	1054	toluene	hexone	0.07	6.80	3.36	0.48
502	1060	toluene	2-pentanone	0.05	0.45	6.25	4.28
501	1051	benzene	acetone	0.17	0.41	1.33	0.89
501	1052	benzene	2-butanone (MEK)	0.36	0.38	1.28	0.56
501	1821	benzene	thiophene	0.04	0.52	1.77	1.17
1864	1403	hexafluorobenzene	diisopropyl ether	0.02	0.13	1.80	0.47
1501	1052	tetrachloromethane	2-butanone (MEK)	0.30	0.27	2.78	1.82
Nonpolar/Weakly Nonpolar Nonideal Systems							
137	1052	cyclohexane	2-butanone (MEK)	0.68	0.69	2.35	1.05
17	1821	heptane	thiophene	0.58	0.44	1.16	0.78
17	1053	heptane	3-pentanone	0.17	0.25	2.38	1.65
17	1052	heptane	2-butanone (MEK)	0.91	0.68	4.74	2.79
56	1051	decane	acetone	0.57	0.83	1.93	1.92
1501	1889	tetrachloromethane	furfural	0.99	1.32	9.10	8.36
1501	1051	tetrachloromethane	acetone	0.18	0.68	1.50	1.39
		average nonpolar/weakly polar		0.36	0.99	2.98	1.97
Nonpolar/Strongly Polar Ideal Systems							
501	1523	benzene	1,2-dichloroethane	0.11	0.11	8.78	0.65
502	1523	toluene	1,2-dichloroethane	0.18	0.33	15.39	0.23
501	1710	benzene	diethylamine	0.10	0.46	3.15	0.51
501	1706	benzene	triethylamine	0.11	0.54	1.04	0.61
504	1774	ethylbenzene	acrylonitrile	2.01	1.54	5.65	5.57
502	1886	toluene	nitrobenzene	0.82	1.59	10.56	2.09
17	1586	heptane	butyl Chloride	0.49	2.08	5.59	1.19
104	1521	cyclopentane	chloroform	0.05	0.14	0.97	0.52
17	1706	heptane	triethylamine	0.01	0.66	0.12	0.10
15	1521	2,3-dimethylbutane	chloroform	0.31	0.37	1.91	0.48
Nonpolar/Strongly Polar Nonideal Systems							
504	1886	ethylbenzene	nitrobenzene	0.35	1.28	1.57	1.49
501	1760	benzene	nitromethane	0.26	1.48	6.56	3.32
501	1108	benzene	<i>tert</i> -butanol	0.46	0.22	6.25	3.24
501	1102	benzene	ethanol	0.65	0.52	2.51	1.55
501	1104	benzene	isopropanol	0.46	1.56	2.90	1.74
17	1682	heptane	ethyl iodide	0.32	1.11	0.90	0.81
137	1791	cyclohexane	pyridine	0.65	0.81	2.50	2.04
27	1791	octane	pyridine	0.17	0.26	1.12	1.07
27	1101	octane	methanol	0.80	0.96	3.33	2.28
137	1102	cyclohexane	ethanol	0.80	0.84	0.78	0.73
7	1105	pentane	1-butanol	1.44	0.97	0.59	0.43
1542	1102	tetrachloroethylene	ethanol	0.61	1.15	8.44	6.31
1864	1103	hexafluorobenzene	1-propanol	0.59	1.97	5.37	2.78
1864	1101	hexafluorobenzene	methanol	1.00	1.04	2.47	1.71
		average nonpolar/strongly polar		0.53	0.92	4.10	1.73
Weakly Polar/Weakly Polar Ideal Systems							
1003	1051	1-propanal	acetone	0.10	0.63	4.61	1.15
1003	1052	1-propanal	butanone	0.36	1.39	7.06	0.7
1051	1321	acetone	vinyl acetate	0.20	0.26	0.82	1.18

Table 4. Continued

system				% AAD P			
ID1	ID2	component 1	component 2	NRTL	PRWS3	SPEADMD	SPEADCI
1051	1314	acetone	propyl acetate	2.07	2.11	4.71	3.05
1002	1321	acetaldehyde	vinyl acetate	0.70	0.77	1.30	1.09
1002	1312	acetaldehyde	methyl acetate	0.68	0.76	2.82	0.98
Weakly Polar/Weakly Polar Nonideal Systems							
1402	1051	diethyl ether	acetone	0.30	0.31	1.61	1.22
1002	1402	acetaldehyde	diethyl ether	0.84	0.96	1.27	1.05
		average nonpolar/strongly polar		0.66	0.90	3.02	1.30
Weakly Polar/Strongly Polar Ideal Systems							
1402	1681	diethyl ether	methyliodide	0.10	1.54	0.92	0.39
1402	1511	diethyl ether	dichloromethane	0.40	0.40	0.63	0.61
1421	1104	1,4-dioxane	isopropanol	0.84	0.65	3.80	3.16
Weakly Polar/Strongly Polar Nonideal Systems							
1415	1521	ethyl propyl ether	chloroform	0.45	1.29	1.79	1.48
1402	1521	diethyl ether	chloroform	0.79	0.88	1.28	1.17
1051	1521	acetone	chloroform	0.38	0.71	2.31	0.89
1314	1103	propyl acetate	1-propanol	0.23	0.21	4.32	3.78
1315	1105	butyl acetate	1-butanol	0.81	1.25	6.73	4.72
1313	1104	ethyl acetate	isopropanol	0.39	0.92	10.41	2.02
1402	1102	diethyl ether	ethanol	0.77	0.83	2.63	2.53
1889	1102	furfural	ethanol	1.95	1.69	2.49	2.25
1051	1101	acetone	methanol	0.09	0.45	1.26	1.20
1421	1101	1,4-dioxane	methanol	0.33	1.01	2.03	2.00
		average weakly polar/strongly polar		0.58	0.91	3.12	2.01
Strongly Polar/Strongly Polar Ideal Systems							
1102	1706	ethanol	triethylamine	0.32	2.90	0.58	0.51
1108	1105	<i>tert</i> -butanol	1-butanol	0.30	0.38	6.75	5.81
1103	1106	1-propanol	isobutanol	0.19	0.80	1.89	1.11
1102	1104	ethanol	isopropanol	0.29	1.39	6.64	2.95
1101	1106	methanol	isobutanol	0.31	0.84	1.05	0.99
1102	1106	ethanol	isobutanol	0.14	0.52	1.82	1.67
Strongly Polar/Strongly Polar Nonideal Systems							
1712	1105	butylamine	1-butanol	0.74	1.52	3.74	3.48
1710	1102	diethylamine	ethanol	2.29	2.06	3.12	2.98
1102	1772	methanol	acetonitrile	0.30	0.37	4.44	4.26
1712	1103	butylamine	1-propanol	0.91	1.73	3.64	3.06
1680	1151	bromobenzene	cyclohexanol	0.17	0.83	1.42	1.07
1523	1106	1,2-dichloroethane	isobutanol	0.45	1.01	10.33	4.02
1101	1523	methanol	1,2-dichloroethane	0.39	1.46	8.02	3.2
		average strongly polar/strongly polar		0.52	1.22	4.11	2.70
Aqueous/Strongly Polar							
1921	1710	water	diethylamine	1.65	2.79	5.92	5.89
1921	1791	water	pyridine	0.72	0.73	2.33	2.12
1921	1101	water	methanol	0.26	1.04	3.43	1.99
1921	1104	water	isopropanol	1.12	1.11	2.92	2.45
1921	1102	water	ethanol	0.76	0.99	1.01	0.91
		average aqueous/strongly polar		0.90	1.33	3.12	2.67
Immiscible Systems							
11	1761	hexane	nitroethane	0.68	2.06	9.56	6.73
12	1761	2-methylpentane	nitroethane	0.63	1.97	12.60	9.83
1761	27	nitroethane	octane	0.27	2.58	45.12	8.21
1101	137	methanol	cyclohexane	1.13	0.43	2.78	2.67
1921	1080	water	cyclohexanone	2.87	1.81	5.53	5.04
1921	1181	water	phenol	3.62	7.65	4.1	3.91
		average immiscible systems		1.53	2.75	13.28	6.06
Carboxylic Acid Systems							
1501	1252	tetrachloromethane	hexoic acid	0.74	0.63	10.31	0.80
1304	1251	butyl formate	formic acid	0.58	4.64	7.48	1.97
1571	1253	chlorobenzene	propionic acid	0.90	1.27	8.35	1.73
1251	1252	formic acid	hexoic acid	0.51	5.05	8.14	1.30
1511	1252	dichloromethane	hexoic acid	1.21	0.68	2.25	2.01
		average carboxylic acid systems		0.79	2.45	7.31	1.56
		overall average		0.57	1.12	4.92	2.31

systems has been reported by Elliott et al. in a related previous report.¹³ That report also includes a detailed analysis of the diethylamine + water system, which is among the Table 3 systems showing relatively large deviations. The value reported

here has been updated from the previous value, but the analysis has not changed fundamentally. The key observation is that diethylamine would behave like pentane if not for the strong solvation interaction. In fact, the pure component properties of

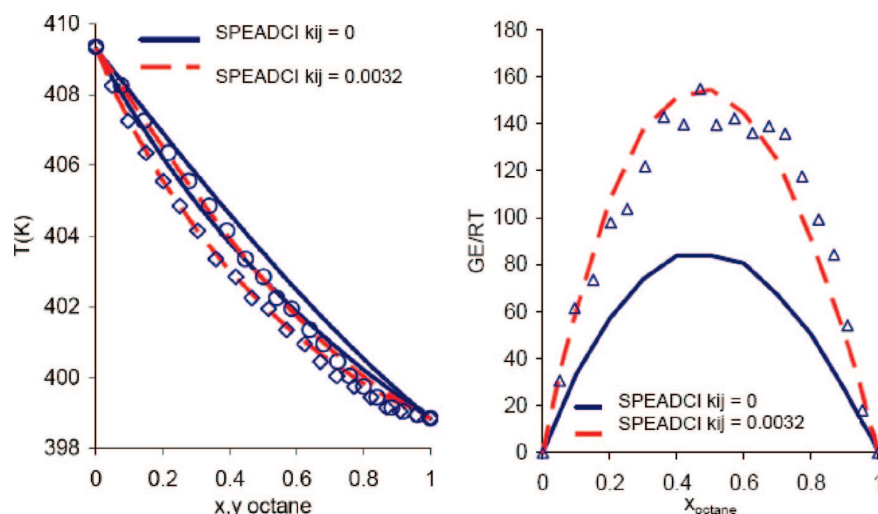


Figure 1. VLE for octane + ethylbenzene at 0.101325 MPa Gibbs excess energy for octane + ethylbenzene, experimental data Δ .¹⁶

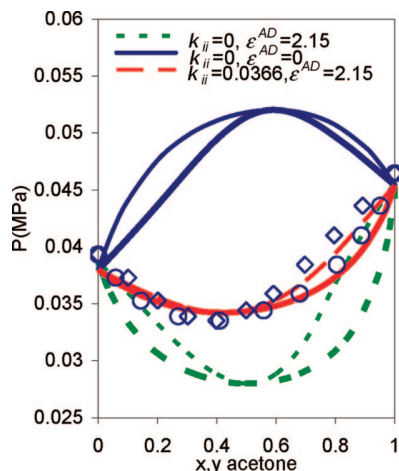


Figure 2. VLE for acetone + chloroform at 308 K. Solvation for acetone $K^{AD} = 0.0025 \text{ nm}^3$, 1.3 kcal/mol, and for chloroform $K^{AD} = 0.0003 \text{ nm}^3$, 3.0 kcal/mol.

diethylamine are somewhat similar to those of pentane. Treating the solvation through the SPEADMD model explains the vast majority of what makes diethylamine different from pentane, but there are still some subtleties that could benefit from a more detailed molecular model.

In addition to the diethylamine + water system, three nitroethane + hydrocarbon systems exhibit large deviations. A typical nitroethane system is illustrated in Figure 3. Note that both SPEADCI and the experimental data indicate LLE in the phase diagram. The best value of k_{ij} that makes the SPEADCI model predict the LLE correctly is 0.063. The experimental mutual solubility are $x_N^U = 0.2388$ and $x_O^L = 0.1478$. The predicted values with the SPEADCI model are $x_N^U = 0.2388$ and $x_O^L = 0.0282$, whereas for the SPEADMD model the mutual solubilities are $x_N^U = 0.2116$ and $x_O^L = 0.0173$. Our current model of nitrates includes weak association of the 2B form. Although this is sufficient to describe the vapor pressure behavior, it may be possible to improve the model. Optimizing the vapor pressure of nitrates with stronger association causes the skewness of this curve to move in the right direction. We intend to include consideration of mixtures as we refine our characterization of nitrate interaction potentials.

Finally, three other systems exhibit large deviations: butyl formate + formic acid, tetrachloromethane + furfural, and

ethylbenzene + acrylonitrile. The system of formic acid + butyl formate is a special case of acid + ester interactions in which formic acid represents the smallest of carboxylic acids and a transferable characterization of acid bonding sites is applied for all carboxylic acids (Figure 4). It may be that the lack of any hydrocarbon content alters formic acid's bonding interactions. More details regarding carboxylic acids will be presented in a forthcoming article devoted to the subject. Figure 5 shows that the boiling temperatures of tetrachloromethane + furfural components are very different ($\sim 100 \text{ K}$) making it very sensitive to the detailed description of the mixing behavior, although the qualitative behavior is well-represented. Lastly, Figure 6 shows that the ethylbenzene + acrylonitrile system has a similar difference between the boiling point temperatures and weak association of the acrylonitrile. Note that we have just begun to characterize the nitrile systems in a transferable way. Similar to nitrate systems, we must include consideration of mixture behavior as a sensitive measure of subtleties in the complexation behavior as we characterize these interactions. We will omit the Danner–Gess systems from the training sets for this analysis such that validations using the Danner–Gess database can reasonably represent predictions.

7. Conclusions

The SPEADMD model can correlate VLE with satisfactory accuracy, but only if the vapor pressure error is small. The SPEADCI compensates for the vapor pressure error and thus is competitive with NRTL and PRWS3 for all systems except the immiscible ones. The SPEADMD and SPEADMDCI models were improved by accounting for the asymmetric Gibbs excess energy (G^{ex}) by adding solvation in several test cases where it was strongly indicated. The solvation is needed because the dispersion interactions alone cannot explain the shape of the G^{ex} curve. The inferred solvation energies are reasonable in comparison to values measured spectroscopically or computed from quantum mechanics.

Several systems still exhibit excessively large deviations, even for the SPEADCI model. These systems require further analysis to understand the peculiar intermolecular forces at work. Nitrates and nitriles are particular examples. The adherence to a molecular model with specific meanings attached to the parameters has limitations in its flexibility to simply correlate data, but also helps to identify solution behavior that deviates from the model assumptions. This identification can help to

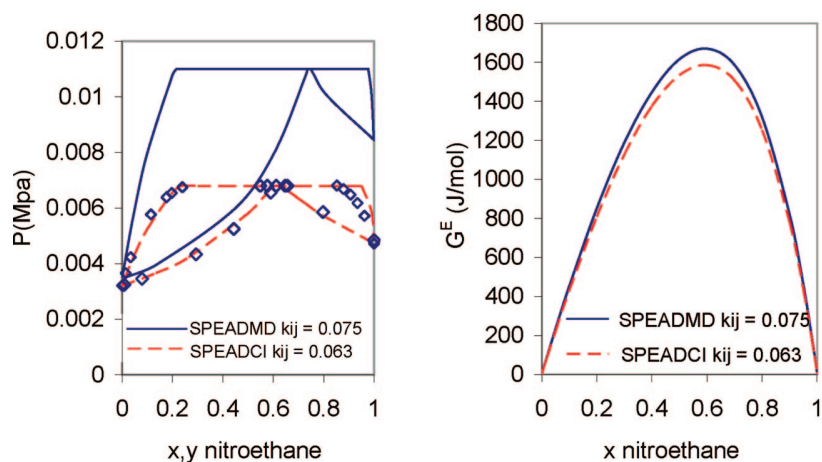


Figure 3. VLE and G^E for nitroethane + octane. Immiscibility causes deviations at high nitroethane compositions. Skewness in G^E is too far to the right.

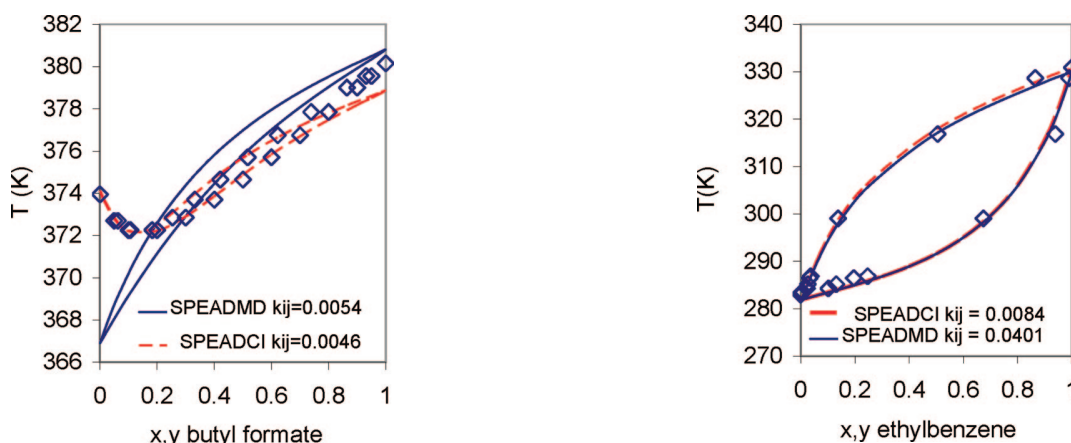


Figure 4. VLE for butyl formate + formic acid system at atmospheric pressure.

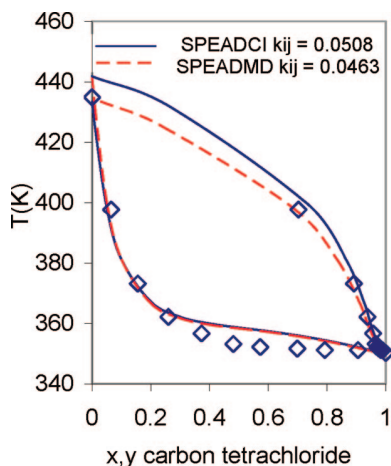


Figure 5. VLE for carbon tetrachloride + furfural at atmospheric pressure.

focus attention for refinements in the model, including subtleties that should help to improve molecular design and chemical formulations.

Overall, the small deviations for the vast majority of systems indicate that the model based on TPT treatment of dispersion forces with Wertheim's hydrogen bonding model is satisfactory. To this extent, inclusion of point charges and explicit charac-

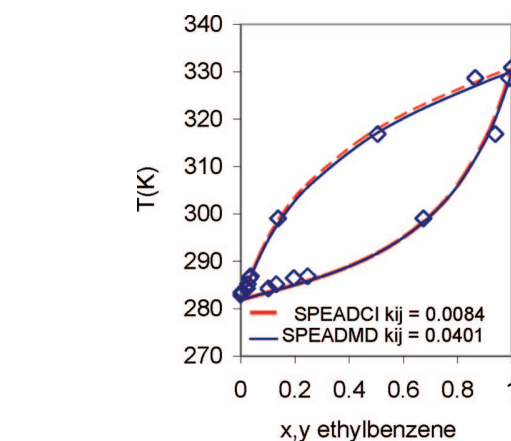


Figure 6. VLE phase diagram for the ethylbenzene + acrylonitrile system at 0.07 bar.

terization of polar moments in the molecular model would appear to be unnecessary. Including additional terms in the model to explicitly treat polarity may help with several of the difficult systems identified above, however, and this will be the subject of future research.

Acknowledgment

This material is based on work supported by the National Science Foundation under Grant CTS-0075883, CTS-0226532, and by Chemstations, Inc., Houston, TX. Any opinions, findings, and conclusions or recommendations expressed in this material are those of the author(s) and do not necessarily reflect the views of the National Science Foundation.

Supporting Information Available: Appendices for the paper (PDF). This material is available free of charge via the Internet at <http://pubs.acs.org>.

Literature Cited

- (1) Orbey, H.; Sandler, S. I., *Modeling Vapor-Liquid Equilibria: Cubic Equations of State and Their Mixing Rules*; Cambridge University Press: New York, 1998.
- (2) Unlu, O.; Gray, N.; Gerek, Z. N.; Elliott, J. R. Transferable Step Potentials for the Straight Chain Alkanes, Alkenes, Alkynes, Ethers, and Alcohols. *Ind. Eng. Chem. Res.* **2004**, *43*, 1788–1793.
- (3) Cui, J., Jr. Phase Diagrams for Multi-Step Potential Models of n-Alkanes by Discontinuous Molecular Dynamics/Thermodynamic Perturbation Theory. *J. Chem. Phys.* **2002**, *116*, 8625.

- (4) Gray, N. H.; Elliott, J. R. In *Quadratic Mixing in Perturbation Theory*, AIChE Fall National Meeting, Austin, TX, 2004; American Institute of Chemical Engineers: New York, 2004; p 160e.
- (5) Danner, R. P.; Gess, M. A. A Database Standard for Evaluation of Vapor-Liquid-Equilibrium Models. *Fluid Phase Equilib.* **1990**, *56*, 285–301.
- (6) Renon, H.; Prausnitz, J. M. Estimation of parameters for the NRTL equation for excess Gibbs energies of strongly nonideal liquid mixtures. *Ind. Eng. Chem. Process. Des. Dev.* **1969**, *8*, 413.
- (7) Abrams, D. S.; Prausnitz, J. M. Statistical Thermodynamics of Liquid Mixtures: A New Expression for the Excess Gibbs Energy of Partly or Completely Miscible Systems. *AIChE J.* **1975**, *21*, 116.
- (8) Fredenslund, A.; Gmehling, J.; Rasmussen, P. *Vapor-Liquid Equilibria Using UNIFAC*; Elsevier Scientific: Amsterdam, 1977.
- (9) Elliott, J. R.; Lira, C. T., *Introductory Chemical Engineering Thermodynamics*; Prentice-Hall: Englewood Cliffs, NJ, 1999; p 660.
- (10) Wong, D. S. H.; Sandler, S. I. A Theoretically Correct Mixing Rule for Cubic Equations of State. *AIChE J.* **1992**, *38*, 671.
- (11) Carnahan, N. F.; Starling, K. E. Equation of State for Nonattracting Rigid Sphere. *J. Chem. Phys.* **1969**, *51*, 635.
- (12) Sans, A. D.; Elliott, J. R. Transferable Potentials For Perfluorinated Molecules. *Fluid Phase Equilib.* **2008**, *263*, 182–189.
- (13) Elliott, J. R.; Vahid, A.; Sans, A. D. Transferable potentials for mixed alcohol-amine interactions. *Fluid Phase Equilib.* **2007**, *256*, 4–13.
- (14) Press, W. H., *Numerical Recipes in Fortran*; 2nd ed.; Cambridge University Press: New York, 1992.
- (15) Ralston, M. L.; Jennrich, R. I. DUD, A Derivative-Free Algorithm for Nonlinear Least Squares. *Technometrics* **1978**, *20*, 7.
- (16) Yang, C. P.; van Winkle, M. Vapor-Liquid Equilibria at Subatmospheric Pressures. *Ind. Eng. Chem.* **1955**, *47*, 293.

Received for review March 6, 2008

Revised manuscript received August 14, 2008

Accepted August 15, 2008

IE800374H